

DDUNet: Dual Dynamic U-Net for Highly-Efficient Cloud Segmentation

Yijie Li¹, Hwei Wang², Jinfeng Xu³, Puzhen Wu⁴, Yunzhong Xiao², Shaofan Wang⁵, Soumyabrata Dev^{4,6}

¹Northwestern University ²Carnegie Mellon University ³The University of Hong Kong

⁴University College Dublin ⁵Beijing University of Technology ⁶The ADAPT SFI Research Centre

Abstract—Cloud segmentation amounts to separating cloud pixels from non-cloud pixels in an image. Current deep learning methods for cloud segmentation suffer from three issues. (a) Constrain on their receptive field due to the fixed size of the convolution kernel. (b) Lack of robustness towards different scenarios. (c) Requirement of a large number of parameters and limitations for real-time implementation. To address these issues, we propose a Dual Dynamic U-Net (DDUNet) for supervised cloud segmentation. The DDUNet adheres to a U-Net architecture and integrates two crucial modules: the dynamic multi-scale convolution (DMSC), improving merging features under different reception fields, and the dynamic weights and bias generator (DWBG) in classification layers to enhance generalization ability. More importantly, owing to the use of depth-wise convolution, the DDUNet is a lightweight network that can achieve 95.3% accuracy on the SWINySEG dataset with only 0.33M parameters, and achieve superior performance over three different configurations of the SWINySeg dataset in both accuracy and efficiency. Our code is publicly available at: <https://github.com/Att100/DDUNet>.

Index Terms—deep learning, cloud segmentation, U-Net, reception field, dynamic convolution

I. INTRODUCTION

Cloud information analysis is necessary and important for meteorology research. The distribution or form of the cloud can reflect specific information that can be used to learn the weather and generate advanced predictions. Generally, cloud images are taken by the meteorological satellite in the near-earth orbit, but in recent years, ground-based sky cameras [1, 2] have been widely used because of their better temporal and spatial resolutions. Several datasets of optical RGB images captured by these sky cameras are released to the community, including SWIMSEG [3], SWINSEG [4], and SWINySEG [5]. With the development of deep neural networks, cloud segmentation for meteorology was further developed. A great number of full convolution network (FCN) [6] and feature pyramid network (FPN) [7] based structures are used for cloud segmentation which consists of a backbone encoder and series of specially designed decoders. However, in recent years, with the development of mobile devices and embedded systems, there is a growing need for a lightweight and efficient model that can perform the segmentation in real-time on those devices. Many previous works have excellent performances, but they usually have large model sizes which makes it hard to perform real-time inference.

In this paper, we introduce Dual Dynamic U-Net (DDUNet) which uses U-Net as fundamental architecture and we proposed Dynamic Multi-scale Convolution (DMSC) in which multiple

depth-wise convolutions with different dilation rates are adopted to increase the reception field and feature extraction ability without too many parameters. We also introduce Dynamic Wights and Bias Generator (DWBG) for our decoders to improve the generalization ability. We evaluate DDUNet on three different configurations, day-time, night-time, and day+night time of the SWINySEG dataset that confirm its effectiveness.

II. RELATED WORKS

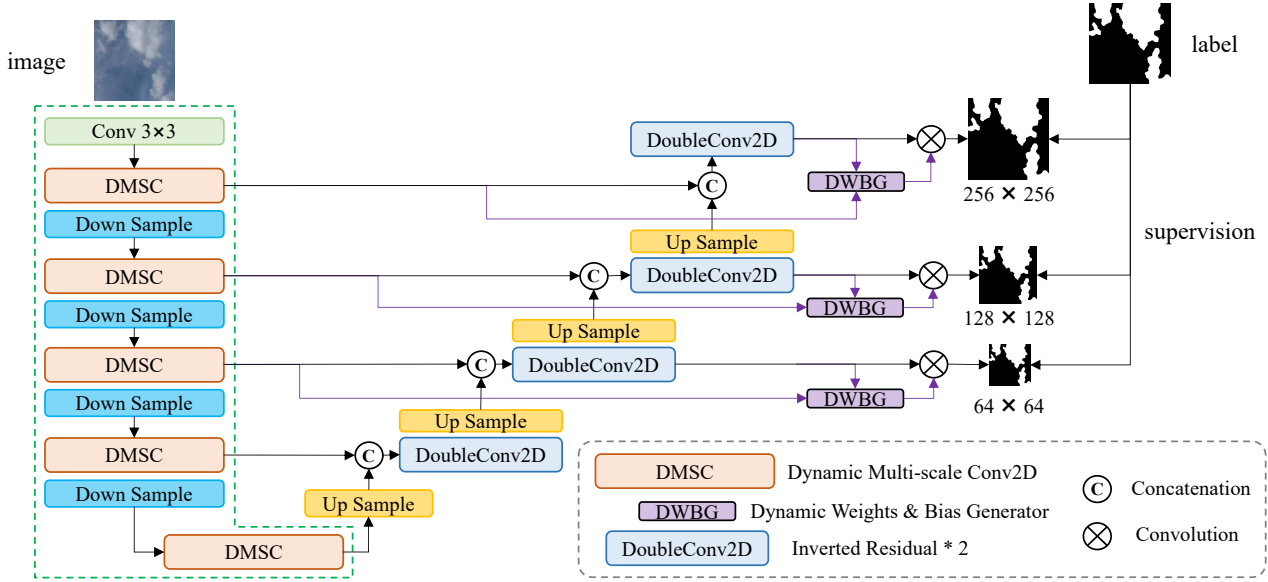
Cloud image segmentation methods can be broadly categorized into traditional approaches [8, 9] and deep learning methods [5, 10]. Traditional methods, such as those by Dev *et al.* [9], utilize color features, fixed convolution filters, and PCA with fuzzy clustering to highlight color differences between clouds and the sky. While effective in capturing overall distributions, these methods often lack detail, leading to lower segmentation accuracy. Deep learning approaches have significantly improved segmentation performance. Dev *et al.* [5] introduced CloudSegNet, an FCN-based method for binary cloud masks, and later expanded to multi-label segmentation[10], classifying images into thin cloud, thick cloud, and sky. Shi *et al.* [11] proposed CloudU-Net, combining U-Net with CRFs for refined segmentation, and enhanced it with dilated convolutions for a larger receptive field. CloudU-NetV2 [12] improved spatial and channel feature optimization using attention mechanisms and employed the RAdam optimizer for better convergence. Recently, Li *et al.* [13] introduced UCloudNet, leveraging U-Net with residual connections and deep supervision for enhanced training. Recent research in remote sensing, such as superpixel-based methods for clustering hyperspectral images [14] and real-time analysis of UAV imagery [15], also underscores the importance of lightweight and scalable architectures in real-world applications. Recent research in remote sensing, such as superpixel-based methods for clustering hyperspectral images [14] and real-time analysis of UAV imagery [15], also underscores the importance of lightweight and scalable learning-based model architectures in real-world applications.

III. ARCHITECTURE

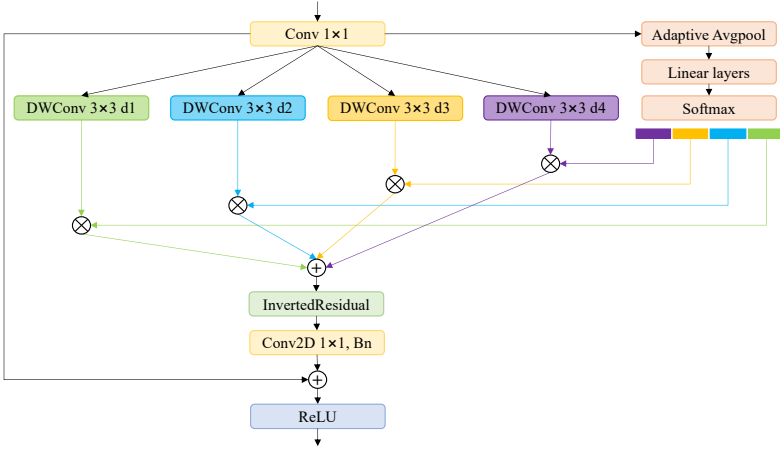
DDUNet is built on the U-Net [16] architecture, consisting of a backbone encoder and four decoders with channel concatenation at each stage, as shown in Figure 1a. Many computer vision works adopt encoder-decoder architectures integrated with CNNs to encode 2D image data [17–19]. Encoder-decoder model architectures are widely applied in autonomous driving [20], medical imaging [21, 22], saliency object detection [23, 24], recommender system [25, 26], and robotics [27–31]. In our work, to enhance feature extraction efficiency, the encoder (green dashed area in Figure 1a) includes four dynamic multi-scale convolution (DMSC) blocks and four stride-2 convolution layers, generating feature maps of sizes 32×32 , 64×64 , 128×128 , and

This research was conducted with the financial support of Science Foundation Ireland under Grant Agreement No. 13/RC/2106_P2 at the ADAPT SFI Research Centre at University College Dublin. The ADAPT Centre for Digital Content Technology is partially supported by the SFI Research Centres Programme (Grant 13/RC/2106_P2) and is co-funded under the European Regional Development Fund.

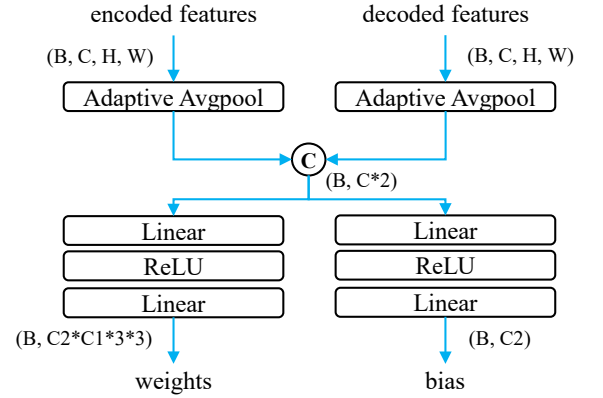
Send correspondence to S. Dev, E-mail: soumyabrata.dev@ucd.ie.



(a) The architecture of the DDUNet model. The structure of sub-modules has been omitted in this figure.



(b) Dynamic Multi-scale Conv2D (DMSC), d_1, d_2, d_3, d_4 indicate the dilation rates of 1, 2, 3, 4. Linear-Layers is a group of layers constructed by (Linear, ReLU, and Linear).



(c) Dynamic Weights and Bias Generator (DWBG).

Fig. 1: Overall Pipeline, DMSC, and DWBG.

256×256 . In the decoder, four blocks progressively upsample feature maps from (H, W) to $(2H, 2W)$ while reducing channels. Each block comprises two inverted residual [32] blocks and one upsample layer. Decoded feature maps pass through dynamic convolution layers with weights and biases generated by a dynamic weights and bias generator (DWBG). Finally, predictions from the last three stages are used for deep supervision to accelerate convergence.

A. Basic Building Blocks

The structures of these sub-modules are shown in Figure 2. In Figure 2 (a), we use a depth-wise convolution layer, batch normalization layer, and a ReLU activation to construct a DW-Conv block for implementation of Dynamic Multi-scale Conv2D (DMSC). The depth-convolution layer means the group of the convolution layer equals the number of input channels that take advantage of group convolution to reduce computation complexity. Figure 2 (b) shows the structure of the Conv block, we use both 1×1 filters and 3×3 filters in DDUNet. Figure 2 (c) shows the structure of Inverted Residual [32]. We use the Inverted Residual block in decoders to further reduce the inference time.

B. Dynamic Multi-scale Conv2D (DMSC)

We propose Dynamic Multi-Scale Conv2D (DMSC), shown in Figure 1b, to enhance multi-scale feature extraction by dynam-

ically aggregating features of different scales. Traditional 1×1 or 3×3 convolutions have limited receptive fields, which hinder small object feature extraction. Dilated convolutions address this by introducing gaps (skip connections) to expand the receptive field. DMSC utilizes four dilation rates to extract features at varying scales. Similar to ASPP [33], which uses different dilation rates, and PSP [34], which uses varied kernel sizes, DMSC improves context aggregation. In our design, a 1×1 Conv block maps input features into a new space, followed by five branches. The first branch applies adaptive average pooling and reshapes the feature map from (B, C, H, W) to $(B, C, 1, 1)$ and then to (B, C) ,

$$F_c = \text{Reshape}(\text{AdptiveAvgPool}(F_{in})) \quad (1)$$

Then we use a series of linear layers to learn a weight vector that will be applied to the four multi-scale feature maps, which can be formulated as:

$$F_{\text{logits}} = \text{Linear}(\text{ReLU}(\text{Linear}(F_c))) \quad (2)$$

Apply softmax activation to retrieve the weight vector W ,

$$W = \text{Softmax}(F_{\text{logits}}) \quad (3)$$

After that, we apply the multi-scale dilated DWConvs to F_{in} , which can be formulated as:

$$F_d^r = \text{DWConv}_{3 \times 3}^r(F_{in}), r \in \{1, 2, 3, 4\} \quad (4)$$

in which, F_d^r indicates the feature map after the convolution with a dilation rate of r . We then apply the weight vector W to $\{F_d^1, F_d^2, F_d^3, F_d^4\}$, which can be given as,

$$F_a = \sum_{r=1}^4 F_d^r * W_r \quad (5)$$

where F_a represents the aggregated feature map, W_r indicates the weight element that will apply to the feature map F_d^r . After that, we use a 3×3 Conv block to extract the feature, F_a' , which can be written as:

$$F_a' = \text{Conv}_{3 \times 3}(F_a) \quad (6)$$

Finally, we apply a short-cut connection together with a 1×1 Conv, inspired by PSPNet [34],

$$F_{out} = \text{ReLU}(\text{BN}(\text{Conv}_{2D_{1 \times 1}}(F_a')) + F_{in}) \quad (7)$$

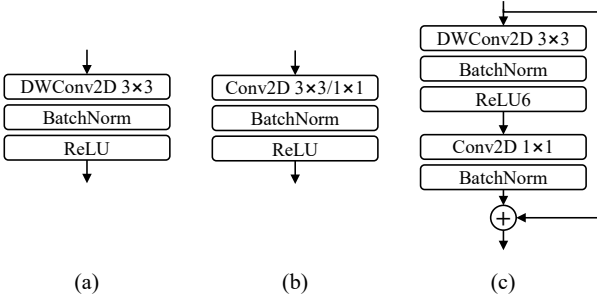


Fig. 2: Basic building blocks used in DDUNet. (a) DWConv block with 3×3 filters; (b) Conv block with 1×1 or 3×3 filters; (c) Inverted Residual [32] without expand ratio.

C. Dynamic Wights & Bias Generator (DWBG)

In most semantic segmentation models, a single Conv2D layer with fixed weights and biases is used for prediction, potentially limiting generalization. To address this, we implement a dynamic convolution layer with a dynamic weight & bias generator (DWBG), as shown in Figure 1. DWBG customizes weights for each input by processing encoder and decoder feature maps. These maps are squeezed using adaptive average pooling, concatenated along the channel axis, and reshaped to $(B, C * 2)$. Two linear layers then generate weights and biases for the convolution operation. The generated weights have a shape of $(B, C_2, C_1, 3, 3)$, where C_1 and C_2 are the input and output channels, respectively.

D. Loss function

We use binary cross entropy as the loss function and the total loss function can be represented as follows:

$$\mathcal{L}_{bce} = -\frac{1}{N} * \sum_{i=0}^N y_i * \log p_i + (1 - y_i) * \log (1 - p_i) \quad (8)$$

$$\mathcal{L}_{total} = \sum_{j=1}^3 \alpha_j * \mathcal{L}_{bce}^j \quad (9)$$

in which, p_i and y_i indicate the i th pixel of the prediction and label. N is the total number of pixels in the prediction map. α_j represent the weight of the loss value of j th decoder block. In our approach, we empirically set $\alpha_1 = 1$, $\alpha_2 = 0.5$ and $\alpha_3 = 0.2$.

IV. EXPERIMENTS & RESULTS

A. Experiments Setting

We follow [38] to split the SWINySEG dataset (contains 6078 day-time cloud images and 690 night-time cloud images) with a ratio of 9:1 for training and testing. The batch size is 16 and the models are trained for 100 epochs. We use Adam with an initialized learning rate of $1e-3$. Exponential learning-rate decay is applied with γ equal to 0.95 after each training epoch. We evaluate our model with four widely used metrics: accuracy, precision, F-measure, and MIoU.

B. Qualitative Analysis

We compare the predictions of the baseline model (lightweight U-Net, 0.32M parameters), DDUNet, and ground truth, as shown in Figure 3. The first six columns are daytime images, and the last six are nighttime. DDUNet produces more complete masks (e.g., columns 3, 6, and 11), correctly segmenting large patches missed by the baseline. It also performs better on small cloud patches (e.g., columns 1 and 3) and reduces false positives in large cloud-labeled areas, improving overall segmentation accuracy.

C. Quantitative Analysis

Quantitative evaluation results of our methods are shown in Table I, which shows the accuracy, precision, F-measure, and MIoU of DDUNet with other methods on day-time, night-time, and day+night time images. DDUNet only has 0.33M parameters which enables the ability to run in very small latency on computational resources-limited devices. By comparing with the current smallest model, the CloudSegNet [5], with only 0.005M parameters achieves 89.6% accuracy on day+night time split and DDUNet has more parameters, but it can achieve 95.3% accuracy on the same split. Because the parameter amount is under 0.5M, the difference in inference latency between the two models can be ignored and the advancement of DDUNet is highlighted. Besides, those methods that have similar performance with DDUNet, such as DeeplabV3+ [36] and CloudU-Net [11] can both achieve 95% accuracy but the parameters number of DDUNet is only 1/9 and 1/100 of them.

D. Ablation Study

We perform an ablation study on model components and parameter sizes, as summarized in Table II. A lightweight U-Net baseline with 0.32M parameters achieves 93.0% accuracy and an MIoU of 0.839. Replacing the baseline encoder with DMSCs reduces parameters to 0.28M while improving accuracy to 94.8% and MIoU to 0.873. Adding DWBGs further boosts DDUNet's performance to 95.3% accuracy and 0.884 MIoU. We also vary model size using the hyperparameter *base_channels* (set to 8 in prior experiments). Reducing it to 4 results in a smaller model, while increasing it to 16 yields limited performance gains, confirming that *base_channels* = 8 achieves an optimal balance between performance and size.

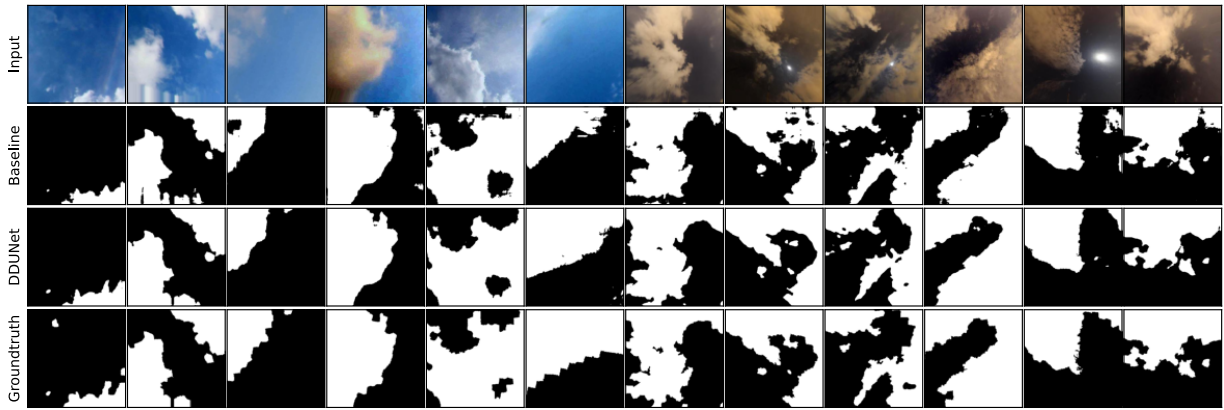


Fig. 3: Results of cloud segmentation for day-time (1-6 columns) and night-time (7-12 columns).

TABLE I: Comparison of DDUNet with other methods on SWINySEG dataset

Methods	#Params (M)	Day-time				Night-time				Day+Night time			
		Acc.	Prec.	mF_{β}	MIoU	Acc.	Prec.	mF_{β}	MIoU	Acc.	Prec.	mF_{β}	MIoU
General Semantic Segmentation Models													
U-Net [16]	24.90	.943	.945	.945	.891	.953	.949	.946	.909	.944	.945	.945	.893
PSPNet [35]	6.92	.945	.953	.948	.896	.938	.927	.929	.882	.945	.951	.946	.895
DeepLabV3+ [36]	2.753	.953	.962	.955	.911	.947	.931	.939	.898	.953	.960	.954	.910
Special Designed Cloud Segmentation Models													
CloudSegNet [5]	0.005	.893	.888	.898	.806	.880	.870	.895	.813	.896	.899	.899	.811
SegCloud [37]	19.61	.941	.953	.943	.889	.955	.936	.948	.912	.942	.952	.944	.891
CloudU-Net [11]	35.49	.954	.956	.956	.912	.954	.925	.949	.912	.954	.954	.956	.913
CloudU-Netv2 [12]	14.55	.940	.967	.941	.887	.954	.931	.948	.911	.941	.964	.941	.889
MA-SegCloud [38]	16.3	.969	.971	.970	.940	.969	.960	.965	.940	.969	.970	.970	.940
Proposed Model													
DDUNet	0.33	.953	.953	.948	.882	.954	.951	.940	.900	.953	.952	.947	.884

No.	Methods	#Params	SWINySEG			
			Acc.	Prec.	mF_{β}	MIoU
1	Baseline	0.32M	.930	.937	.925	.839
2	No. 1+DMSC	0.28M	.948	.943	.942	.873
3	No. 2+DWBG	0.33M	.953	.952	.947	.884
5	No. 3 (0.27x)	0.09M	.936	.933	.932	.849
6	No. 3 (3.79x)	1.25M	.954	.955	.947	.886

TABLE II: Ablation study on different module compositions and different scaling on parameters amount

V. CONCLUSION AND DISCUSSION

In this paper, we introduce the dual dynamic U-Net (DDUNet) for cloud segmentation aiming to achieve a balance between accuracy and efficiency. By introducing dynamic multi-scale convolution (DMSC), DDUNet can extract the features of cloud patches with different scales and adaptive merge the feature maps. The dynamic weights and bias generator (DWBG) adaptive generates weights and bias for the final classification layer which enhances generalization ability across various scenarios. Significantly, its use of depth-wise convolution renders the DDUNet lightweight, achieving high accuracy (95.3%) on the SWINySEG dataset with minimal parameters (0.33M).

REFERENCES

- [1] M. Jain, I. Gollini, M. Bertolotto, G. McArdle, and S. Dev, "An extremely-low cost ground-based whole sky imager," in *Proc. IEEE International Geoscience and Remote Sensing Symposium (IGARSS)*. IEEE, 2021, pp. 8209–8212.
- [2] S. Dev, F. M. Savoy, Y. H. Lee, and S. Winkler, "Design of low-cost, compact and weather-proof whole sky imagers for high-dynamic-range captures," in *Proc. IEEE International Geoscience and Remote Sensing Symposium (IGARSS)*. IEEE, 2015, pp. 5359–5362.
- [3] S. Dev, Y. H. Lee, and S. Winkler, "Color-based segmentation of sky/cloud images from ground-based cameras," *IEEE Journal of Selected Topics in Applied Earth Observations and Remote Sensing*, vol. 10, no. 1, pp. 231–242, 2016.

- [4] S. Dev, F. M. Savoy, Y. H. Lee, and S. Winkler, "Nighttime sky/cloud image segmentation," in *Proc. IEEE International Conference on Image Processing (ICIP)*. IEEE, 2017, pp. 345–349.
- [5] S. Dev, A. Nautiyal, Y. H. Lee, and S. Winkler, "Cloudsegnet: A deep network for nychthemeron cloud image segmentation," *IEEE Geoscience and Remote Sensing Letters*, vol. 16, no. 12, pp. 1814–1818, 2019.
- [6] J. Long, E. Shelhamer, and T. Darrell, "Fully Convolutional Networks for Semantic Segmentation," in *Proceedings of the IEEE/CVF Conference on Computer Vision and Pattern Recognition (CVPR)*, 2015, pp. 3431–3440.
- [7] T.-Y. Lin, P. Dollár, R. Girshick, K. He, B. Hariharan, and S. Belongie, "Feature pyramid networks for object detection," in *Proceedings of the IEEE conference on computer vision and pattern recognition*, 2017, pp. 2117–2125.
- [8] C. N. Long, J. M. Sabburg, J. Calbó, and D. Pagès, "Retrieving cloud characteristics from ground-based daytime color all-sky images," *Journal of Atmospheric and Oceanic Technology*, vol. 23, no. 5, pp. 633–652, 2006.
- [9] S. Dev, Y. H. Lee, and S. Winkler, "Systematic study of color spaces and components for the segmentation of sky/cloud images," in *Proc. IEEE International Conference on Image Processing (ICIP)*. IEEE, 2014, pp. 5102–5106.
- [10] S. Dev, S. Manandhar, Y. H. Lee, and S. Winkler, "Multi-label cloud segmentation using a deep network," in *2019 USNC-URSI Radio Science Meeting (Joint with AP-S Symposium)*. IEEE, 2019, pp. 113–114.
- [11] C. Shi, Y. Zhou, B. Qiu, D. Guo, and M. Li, "CloudU-Net: A Deep Convolutional Neural Network Architecture for Daytime and Nighttime Cloud Images' Segmentation," *IEEE Geoscience and Remote Sensing Letters (GRSL)*, vol. 18, no. 10, pp. 1688–1692, 2020.

- [12] C. Shi, Y. Zhou, and B. Qiu, "CloudU-Netv2: A Cloud Segmentation Method for Ground-Based Cloud Images Based on Deep Learning," *Neural Processing Letters*, vol. 53, no. 4, pp. 2715–2728, 2021.
- [13] Y. Li, H. Wang, S. Wang, Y. H. Lee, M. S. Pathan, and S. Dev, "UCloudNet: A Residual U-Net with Deep Supervision for Cloud Image Segmentation," in *IGARSS 2024-2024 IEEE International Geoscience and Remote Sensing Symposium*. IEEE, 2024, pp. 5553–5557.
- [14] K. Cui, R. Li, S. L. Polk, Y. Lin, H. Zhang, J. M. Murphy, R. J. Plemmons, and R. H. Chan, "Superpixel-based and Spatially-regularized Diffusion Learning for Unsupervised Hyperspectral Image Clustering," *IEEE Transactions on Geoscience and Remote Sensing*, 2024.
- [15] K. Cui, W. Tang, R. Zhu, M. Wang, G. D. Larsen, V. P. Pauca, S. Alqahtani, F. Yang, D. Segurado, P. Fine *et al.*, "Real-Time Localization and Bimodal Point Pattern Analysis of Palms Using UAV Imagery," *arXiv preprint arXiv:2410.11124*, 2024.
- [16] O. Ronneberger, P. Fischer, and T. Brox, "U-net: Convolutional networks for biomedical image segmentation," in *Proc. International Conference on Medical image computing and computer-assisted intervention*. Springer, 2015, pp. 234–241.
- [17] H. Wang, Y. Li, S. Xi, S. Wang, M. S. Pathan, and S. Dev, "AMDCNet: An attentional multi-directional convolutional network for stereo matching," *Displays*, vol. 74, p. 102243, 2022.
- [18] H. Wang, M. S. Pathan, and S. Dev, "Stereo Matching Based on Visual Sensitive Information," in *2021 6th International Conference on Image, Vision and Computing (ICIVC)*, 2021, pp. 312–316.
- [19] S. Batra, H. Wang, A. Nag, P. Brodeur, M. Checkley, A. Klinkert, and S. Dev, "DMCNet: Diversified model combination network for understanding engagement from video screengrabs," *Systems and Soft Computing*, vol. 4, p. 200039, 2022.
- [20] H. Wang, B. Zhu, Y. Li, K. Gong, Z. Wen, S. Wang, and S. Dev, "SYGNet: A SVD-YOLO based GhostNet for Real-time Driving Scene Parsing," in *2022 IEEE International Conference on Image Processing (ICIP)*, 2022, pp. 2701–2705.
- [21] W. Tang, K. Cui, and R. H. Chan, "Optimized Hard Exudate Detection with Supervised Contrastive Learning," in *2024 IEEE International Symposium on Biomedical Imaging (ISBI)*. IEEE, 2024, pp. 1–5.
- [22] F. Pan, Y. Wu, K. Cui, S. Chen, Y. Li, Y. Liu, A. Shakoor, H. Zhao, B. Lu, S. Zhi *et al.*, "Accurate detection and instance segmentation of unstained living adherent cells in differential interference contrast images," *Computers in Biology and Medicine*, vol. 182, p. 109151, 2024.
- [23] Y. Li, H. Wang, Z. Li, S. Wang, S. Dev, and G. Zuo, "DAANet: Dual Attention Aggregating Network for Salient Object Detection," in *IEEE International Conference on Robotics and Biomimetics (ROBIO)*. IEEE, 2023, pp. 1–7.
- [24] Y. Li, H. Wang, and A. Katsaggelos, "CPDR: Towards Highly-Efficient Salient Object Detection via Crossed Post-decoder Refinement," in *35th British Machine Vision Conference 2024, BMVC 2024, Glasgow, UK, November 25-28, 2024*. BMVA, 2024.
- [25] J. Xu, Z. Chen, J. Li, S. Yang, H. Wang, and E. C. Ngai, "AlignGroup: Learning and Aligning Group Consensus with Member Preferences for Group Recommendation," in *Proceedings of the 33rd ACM International Conference on Information and Knowledge Management*, 2024, pp. 2682–2691.
- [26] J. Xu, Z. Chen, S. Yang, J. Li, H. Wang, and E. C.-H. Ngai, "MENTOR: Multi-level Self-supervised Learning for Multimodal Recommendation," *arXiv preprint arXiv:2402.19407*, 2024.
- [27] Z. Li, H. Wang, Y. Li, S. Dev, and G. Zuo, "VGRISys: A Vision-Guided Robotic Intelligent System for Autonomous Instrument Calibration*," in *2023 IEEE International Conference on Robotics and Biomimetics (ROBIO)*, 2023, pp. 1–6.
- [28] M. Huo, Z. Zhang, X. Ren, X. Yang, and C. Ye, "AbHE: All Attention-Based Homography Estimation," *IEEE Transactions on Instrumentation and Measurement*, vol. 73, pp. 1–11, 2024.
- [29] X. Zhu, R. Tian, C. Xu, M. Huo, W. Zhan, M. Tomizuka, and M. Ding, "Fanuc manipulation: A dataset for learning-based manipulation with fanuc mate 200id robot," 2023.
- [30] Z. Wang, B. Li, C. Wang, and S. Scherer, "AirShot: Efficient Few-Shot Detection for Autonomous Exploration," in *IEEE/RSJ International Conference on Intelligent Robots and Systems (IROS)*, 2024. [Online]. Available: <https://arxiv.org/pdf/2404.05069.pdf>
- [31] Z. Wang, "ONLS: OPTIMAL NOISE LEVEL SEARCH IN DIFFUSION AUTOENCODERS WITHOUT FINE-TUNING," in *The Second Tiny Papers Track at ICLR 2024*, 2024. [Online]. Available: <https://openreview.net/forum?id=Q8diCUHTZd>
- [32] M. Sandler, A. Howard, M. Zhu, A. Zhmoginov, and L.-C. Chen, "Mobilenetv2: Inverted residuals and linear bottlenecks," in *Proceedings of the IEEE conference on computer vision and pattern recognition*, 2018, pp. 4510–4520.
- [33] L.-C. Chen, G. Papandreou, I. Kokkinos, K. Murphy, and A. L. Yuille, "Deeplab: Semantic image segmentation with deep convolutional nets, atrous convolution, and fully connected crfs," *IEEE transactions on pattern analysis and machine intelligence*, vol. 40, no. 4, pp. 834–848, 2017.
- [34] H. Zhao, J. Shi, X. Qi, X. Wang, and J. Jia, "Pyramid scene parsing network," in *Proceedings of the IEEE conference on computer vision and pattern recognition*, 2017, pp. 2881–2890.
- [35] —, "Pyramid Scene Parsing Network," in *Proceedings of the IEEE Conference on Computer Vision and Pattern Recognition (CVPR)*, July 2017.
- [36] L.-C. Chen, G. Papandreou, F. Schroff, and H. Adam, "Rethinking Atrous Convolution for Semantic Image Segmentation," *arXiv preprint arXiv:1706.05587*, 2017.
- [37] W. Xie, D. Liu, M. Yang, S. Chen, B. Wang, Z. Wang, Y. Xia, Y. Liu, Y. Wang, and C. Zhang, "SegCloud: A novel cloud image segmentation model using a deep convolutional neural network for ground-based all-sky-view camera observation," *Atmospheric Measurement Techniques*, vol. 13, no. 4, pp. 1953–1961, 2020.
- [38] L. Zhang, W. Wei, B. Qiu, A. Luo, M. Zhang, and X. Li, "A Novel Ground-Based Cloud Image Segmentation Method Based on a Multibranch Asymmetric Convolution Module and Attention Mechanism," *Remote Sensing*, vol. 14, no. 16, p. 3970, 2022.